

# Analysis of Internal Energy in GFL-MMCs and a Decoupled Energy Control Scheme

Pengxiang Huang and Luigi Vanfretti  
Depart. Electrical, Computer, and Systems Engineering  
Rensselaer Polytechnic Institute  
Troy, NY, 12180, U.S.A  
huangp2@rpi.edu, vanfrl@rpi.edu

**Abstract**—Modular multilevel converters (MMC) with energy-based control schemes have attracted much attention recently. The majority of the proposed control schemes involve making use of the MMC’s internal energy to improve the performance of grid-forming/grid-following (GF-/GFL-) functions in steady state or in preventing disturbance propagation between ac and dc side. Yet, the close coupling between the internal energy-related dynamics of an MMC and its ac side stability characteristics has not been addressed. This paper presents a novel energy-based control scheme that decouples the internal energy-related dynamics of a GFL-MMC from its external energy-related control functions (i.e. dc voltage control, active power control). The proposed control scheme can be applied in MMC-based converters, such as STATCOM, HVDC, etc. Time-domain simulation results are presented and demonstrate functionality of the proposed decoupled energy control scheme. Finally, a frequency-domain model of an MMC w.r.t. the closed-loop output impedance of GFL-MMC is presented, which shows that its external characteristic is not influenced by internal energy-related dynamics.

**Index Terms**—modular multilevel converter, energy-controlled MMC, energy balancing, decoupled control, internal dynamics

## I. INTRODUCTION

MODULAR multilevel converters (MMCs) have become widely considered as the preferable technology of medium-/high- voltage applications in power electronics converter-based power system [1], [2]. Most of the MMCs in commission are controlled by non-energy based schemes [3], [4]. Recently, however, it is revealed that energy-controlled MMCs have better dynamic performance (i.e. response to transients) during normal and abnormal operation than non-energy-controlled MMCs [5], [6]. Two energy balancing objectives are required for energy-controlled MMCs: 1) horizontal balancing: the balancing of per-phase stored energy  $w_{\Sigma}^x (=w_u^x + w_l^x)$  among three phases; 2) vertical balancing (also known as intra-arm balancing): the balancing of per-arm stored energy within one phase, which is related to the energy difference  $w_{\Delta}^x (=w_u^x - w_l^x)$  between upper and lower arm. In the variables above,  $x$  designates phase (a, b, and c), and the subscript  $u/l$  indicates upper and lower arm.

Recent studies over the last five years focus on using energy control schemes to improve MMCs’ dynamic performance during transient and abnormal operation conditions (i.e. unsymmetrical operation, ac faults, etc.). Different energy control schemes for MMCs with a stiff dc-bus, for example grid-forming MMC (GF-MMC), has been comprehensively

investigated in [7], [8]. Unlike GF-MMC, dc-bus voltage in a grid following MMC (GFL-MMC) is not imposed, and needs to be regulated. It is not rational to apply the *classic* horizontal balancing controller used in GF-MMC to GFL-MMC with a dc voltage controller as both control functions involve the dynamic of the common mode current. When both functions are enabled, this will lead to a conflict between the control objectives and potentially instability. Additionally, the dc-bus of GFL-MMC exhibits a stiff current source characteristic, thus any horizontal balancing schemes that assume a manageable dc-bus current will fail in GFL-MMC. To address this issue, per-phase stored energy of GFL-MMC should be controlled to its reference command by regulating the active current of ac grid [6], [9], then the dc voltage can be automatically maintained at  $V_{dc}$ . This method is regarded as the *classic* horizontal balancing method for GFL-MMC, but it may result in poor dynamic performance during operation. For example, any change in ac current of MMC (i.e unbalanced faults) will make horizontal balancing challenging and could result in propagation of the disturbance to the dc side voltage. To resolve this, [10] and [11] swap the roles of ac current and circulating current in regulation of dc voltage and horizontal balancing by using a *cross* control structure. Consequently, MMC is capable of preventing ac disturbance propagation to the dc side during abnormal operation.

It is also reported that sub-synchronous and near-synchronous oscillations (SSO/NSO) interacting with the ac grid can appear in GFL-MMCs due to their internal energy-related dynamics [12], [13]. The root cause is that the internal energy-related dynamics result in two resonant peaks on MMC’s closed-loop output impedance within the SSO/NSO ranges, making it likely to interact with the grid impedance and result in SSO/NSO [13], [14]. Part of the motivation for this work is to use energy regulation to reshape MMC stability characteristics in the frequency range associated with internal energy-related dynamics, which are closely linked to circulating current control and the energy stored in the distributed submodule (SM) capacitors. In addition, as noted in [3], [15], the internal energy-related dynamics create a close coupling between the circulating current controller and other controllers that assist with power transfer functions (i.e. ac/dc voltage control, ac current control, active power controller), that may result in interactions between circulating current

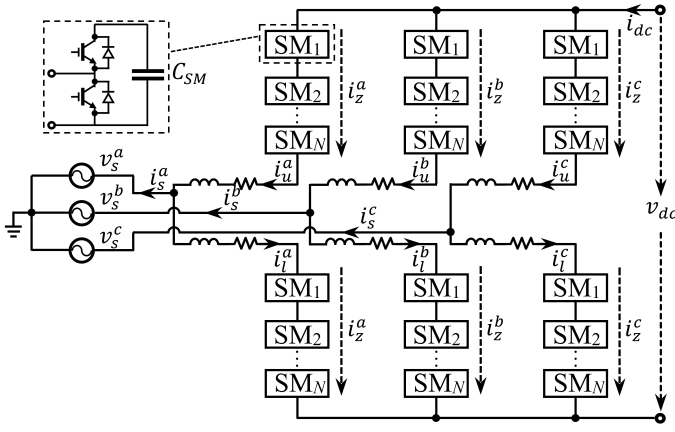


Fig. 1. Circuit diagram of grid-following MMC against an ideal ac grid

control and other controllers.

In this context, there is a clear need to eliminate the MMC's internal energy-related dynamics from their external characteristic by using energy control, which has not been addressed fully in the literature. Consequently, the aim of this paper is to provide a method by which the internal energy-related dynamics of MMC can be fully decoupled from its external characteristic. In contrast to [6], [9]–[11], the proposed energy control scheme for GFL-MMC herein maintains a classic two-level VSC (2L-VSC) control structure in order to avoid unwanted transient behaviors as noted in [10].

The remainder of this article is organized as follows. Section II briefly reviews energy dynamics of a GFL-MMC as well as its *classic* energy control schemes (based upon [6], [9]). Section III presents the proposed decoupled energy control scheme as well as its closed-loop control block diagram. Section IV validates the effectiveness of the proposed energy control scheme through time-domain simulations and frequency-domain analysis. Section V concludes the work.

## II. ENERGY DYNAMICS OF GFL-MMC

Fig. 1 shows a simplified schematic of a three-phase GFL-MMC including six arms, each arm consists of  $N$  sub-modules (SM) with a capacitance  $C_{SM}$ . For brevity, the process of averaging the switched MMC model is disregarded, and the resulting averaged model presented in [16] are used next.

### A. Classic Horizontal Energy Balancing for GFL-MMCs

The *classic* horizontal balancing is achieved by adjusting the per-phase stored energy to its reference command. The dynamic model of MMC per-phase stored energy is given as

$$\frac{dw_{\Sigma}^x}{dt} = \frac{d(w_u^x + w_l^x)}{dt} = v_{dc}i_z^x - \frac{\hat{V}_s \hat{I}_s}{2} \cos \varphi \quad (1)$$

where  $z$  represents the common mode current in each phase,  $s$  the ac grid side variables,  $v_{dc}$  the dc-bus voltage,  $\hat{V}_s$  and  $\hat{I}_s$  the peak value of ac side voltage and current. This notation will be used in the remainder of this paper.

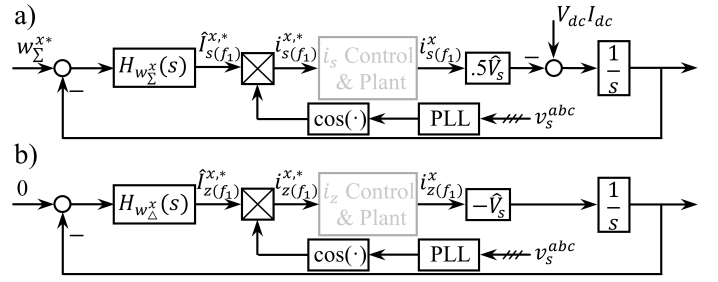


Fig. 2. Block diagram of: a) *classic* horizontal balancing; b) *classic* vertical balancing control for grid-following MMC

It is generally accepted that  $\hat{V}_s$  and dc input power  $v_{dc}i_{dc}$  are not controlled by GFL-MMC, and are assumed constant during steady state operation [9]. To control the per-phase stored energy, *classic* horizontal balancing scheme forms the control structure depicted in Fig. 2 a), consisting of an inner ac current control loop ( $i_s$  control) to adjust  $\hat{I}_s \cos \varphi$ . Note that, as long as the per-phase stored energy is kept to the reference value  $w_{\Sigma}^{x*} = C_{sm} V_{dc}^2 / (2N)$ , the dc voltage will be  $V_{dc}$  and the horizontal energy balancing among three phases inherently achieved. It can be observed that the GFL-MMC will adjust its ac side output power to compensate for any variation in its per-phase stored energy, implying that the ac side output power and the internal stored energy are closely coupled.

### B. Classic Vertical Energy Balancing for GFL-MMCs

The dynamics resulting from the energy imbalance between the upper and lower arms in each phase is given by (2)

$$\frac{dw_{\Delta}^x}{dt} = v_{dc} \hat{I}_s \cos(\omega_1 t - \varphi) - 2\hat{V}_s i_z^x \cos(\omega_1 t - \varphi) \quad (2)$$

It has been the conventional wisdom that a sinusoidal component at fundamental frequency has to be purposely injected into the common mode current  $i_z^x$  in each phase through circulating current control ( $i_z$  control) to compensate the non-zero component existing in  $w_{\Delta}^x$ . Fig. 2 b) presents the vertical energy balancing scheme block diagram. This scheme is used for both grid-forming and grid-following MMCs. As this paper discusses a new control scheme in the horizontal direction, the classic control scheme for the vertical balancing is preserved in the sequel.

## III. DECOUPLED ENERGY CONTROL FOR GFL-MMCs

In order to decouple internal energy- and external energy-related dynamics by control, it is necessary to identify control variables responsible for them. In fact, the per-phase common mode current can be decomposed into three parts as shown

$$i_z^x = \underbrace{i_{dc}/3 + i_{c(dc)}^x}_{dc} + \underbrace{i_{c(f_1)}^x}_{fundamental} \quad (3)$$

where the first term in the right-hand side represents the dc-bus current equally distributed among three phases of MMC, regulating the balancing of (active) power inflow to MMC from dc-bus and outflow from MMC to ac grid. This term

is essentially irrelevant to MMC internal energy; the second term  $i_{c(dc)}^x$  is a dc current circulating only within the three phases, which can be used to compensate the difference of per-phase stored energy between the phases. This term directly determines inter-phase balancing, without specifying how much energy is stored in each phase. However, this term has not caught the attention in [6]–[9], because the *classic* energy control applied to the dc component of  $i_z^x$  in-essence regulates both  $i_{dc}/3$  and  $i_{c(dc)}^x$  simultaneously. In addition, the third term refers to the component used for intra-arm balancing as discussed in Section II.B. Consequently, if a voltage excursion or potentially an instability on the dc-bus is neglected, the MMC internal energy balancing can be achieved by controlling  $i_{c(dc)}^x$  for inter-phase balancing and  $i_{c(f_1)}^x$  for intra-arm balancing. Moreover, once the GFL-MMC has achieved this internal energy balancing, it serves as an energy buffer clamped between the ac and dc side, similar to the large capacitor in a 2L-VSC.

### A. Total Stored Energy Control

Assume an MMC has achieved the internal energy balance by adjusting  $i_{c(dc)}^x$  and  $i_{c(f_1)}^x$ . Since the MMC will now act as an energy buffer, any power imbalance between the ac and dc sides will charge or discharge the buffer, causing uncontrolled variations (potentially instability) of dc-bus voltage. To maintain a constant dc voltage a total stored energy control is proposed below, which regulates the energy stored in six arms to a fixed value. Ignoring power losses in the MMC, the dynamics of total stored energy in MMC can be expressed as:

$$\frac{dE_{tot}}{dt} = v_{dc}i_{dc} - \frac{3}{2}v_s i_s = v_{dc}i_{dc} - \frac{3}{2}v_s^d i_s^d \quad (4)$$

where  $E_{tot}$  represents the total energy stored in all six arms. Note that when the MMC is working in grid-following mode, the average power at the dc-side  $v_{dc}i_{dc}$  and the ac side voltage  $v_s$  (equivalently  $v_s^d$  in the  $dq$ -reference frame) are exogenous variables. Hence, it is intuitive to regulate the total-stored energy in the six arms of MMC through a feedback loop, comparing  $E_{tot}$  with its reference and adjusting accordingly  $i_s^d$  (grid active current in the  $dq$ -reference frame). As a result, the compensation provided by  $i_s^d$  at the ac side eliminates the power imbalance between dc and ac side. As it is desired that the dc offset of the arm voltage is at nominal value  $V_{dc}$  and the effective per-arm capacitance is  $C_{SM}/N$ , the total stored energy in the MMC should be maintained at  $3V_{dc}^2/(2N)$ , which is used as the reference for the total energy control,  $E_t^*$ . Fig. 3 a) shows the block diagram of the proposed total stored energy controller. The closed-loop transfer function is composed of the total stored energy compensator  $H_{E_t}(s)$ , closed-loop grid active current control and the “plant” for total stored energy control  $G_{E_t}(s) = 1.5\hat{V}_s^d/s$ . It may be noted that the proposed control structure is similar to the traditional dc voltage control in non-energy controlled MMCs and 2L-VSCs, where the outer loop ensures a stable dc voltage and its controller’s output is used as a reference for the grid active current controller.

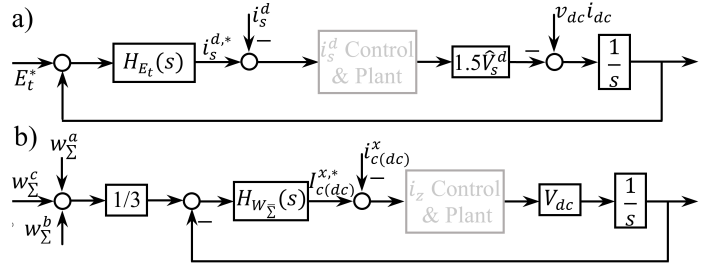


Fig. 3. Block diagram of: a) total stored energy control; b) *modified* horizontal balancing control for grid-following MMC.

### B. Modified Horizontal Energy Balancing

The horizontal energy balancing between phases can now be achieved by regulating  $i_{c(dc)}^x$  in the circulating current of each phase. Thus, the output of the *modified* horizontal energy balancing controller should be used as the dc reference command  $i_{c(dc)}^{x,*}$  driving the circulating current controller. When the per-phase stored energy of three phases are not balanced, the compensated dc circulating current will flow into the phase whose total energy is lower than  $i_{c(dc)}^{x,*}$  and flows out of the phase with higher stored energy than  $i_{c(dc)}^{x,*}$ .

Observe that the only objective here is to balance the energy between three phases, rather than to regulate the per-phase stored energy to any specific required value. If a constant reference command is used, this will create a conflict with the proposed total stored energy controller. Consequently, the set point for this *modified* horizontal balancing controller is modified to one-third of the sum of instantaneous per-phase stored energy. In essence, this controller ensures equal distribution of total stored energy across three phases. The dynamic model for this controller is given as

$$\frac{d(w_\Sigma^a + w_\Sigma^b + w_\Sigma^c)}{dt} = 3V_{dc}(i_{c(dc)}^a + i_{c(dc)}^b + i_{c(dc)}^c). \quad (5)$$

As it can be seen, Equation (5) holds if and only if the dc-bus voltage is kept at  $V_{dc}$ , which highlights the importance of the proposed total stored energy controller discussed earlier. The question may arise as to why total stored energy controller is necessary here rather than classic dc-bus voltage controller to maintain dc voltage. This is due to the fact that classic dc-bus voltage control implicitly engages in the process of regulating  $i_{c(dc)}^x$ . Moreover, note that this *modified* horizontal energy balancing control can be made slower than the total stored energy controller, which allows to separate the time-scales for each control objective. Fig. 3 b) shows the complete block diagram of the *modified* horizontal balancing controller. The closed-loop transfer function consists of the *modified* horizontal balancing compensator  $H_{w_\Sigma}(s)$ , the closed-loop circulating current controller ( $i_z$  control), and the “plant” for the *modified* horizontal balancing controller  $G_{w_\Sigma}(s) = V_{dc}/s$ . Recall that the *classic* vertical balancing control used in GFL-MMC is unchanged from [6], as discussed earlier.

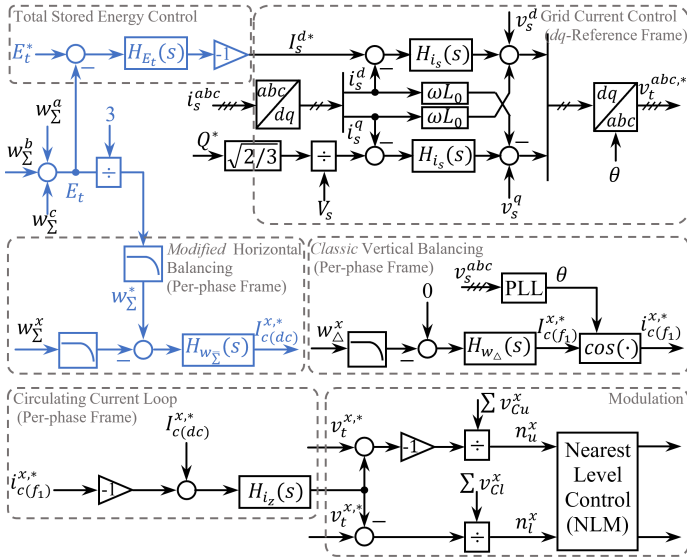


Fig. 4. Detailed control scheme for the energy-controlled GFL-MMC

### C. Overall Control Architecture

The overall control architecture is depicted in Fig. 4, with the control schemes proposed in subsections III.A and III.B shown in blue. All the energy controllers, including  $H_{E_t}(s)$ ,  $H_{w_{\Sigma}^x}(s)$  and  $H_{i_z}(s)$  consist of PI compensators for which different bandwidths are needed. As the total stored energy controller regulates dc-bus voltage, its bandwidth can be set to match that of classic dc-bus voltage controllers used in non-energy controlled-MMC or 2L-VSCs, usually ranging from 5 Hz to 20 Hz. Because energy balancing between arms and phases rely on the change of SM capacitor voltages, which is slow, the *modified* horizontal energy balancing and energy difference control can be designed, but not limited, to give a lower cut-off frequency than total energy control. As  $w_{\Sigma}^x$  and  $w_{\Delta}^x$  ( $x = a, b, c$ ) contain significant 2nd-order harmonics and the fundamental component, respectively, low-pass filters are used to retain the average components necessary for the energy control purposes.

## IV. VALIDATION OF CONTROLLER PERFORMANCE

To validate the proposed energy control design, a case study with time-domain simulation is presented next to show the effectiveness of the proposed control. In addition, the second part of this section aims to verify the decoupling efficacy by using frequency-domain analysis.

The detailed simulation model used represents a 900 MW GFL-MMC (ac: 50Hz/300 kV, dc:  $\pm 320$  kV) [17], with 50 mH and  $0.1 \Omega$  arm inductors and resistances, respectively. The MMC is assumed capable of performing its computation and switching process with an effective time delay of  $200 \mu s$ . The simulation makes use of an ideal current source to model the dc side power source of GFL-MMC. As mentioned before, PI regulators are used for all control functions in this work. Table. I summarizes the design specification in terms of bandwidth and phase margin of controllers. Note that, the

SM capacitor voltages are well-balanced by using the NLC technique proposed in [18].

TABLE I  
CONTROL DESIGN OF ENERGY-CONTROLLED MMC

Control Function	Cut-off Freq.	Phase Margin
AC Current	200 Hz	45°
Circulating Current	300 Hz	45°
Phase-Lock Loop	20 Hz	45°
Total-stored Energy	15 Hz	45°
<i>Modified Hori. Balancing</i>	15 Hz	45°
<i>Classic Vertical Balancing</i>	5 Hz	45°

### A. Time-domain Simulation Results

In order to ensure stable operation of the GFL-MMC, the simulation starts with only total stored energy control, ac current control, and phase-locked loop control conducted. As can be seen from Fig. 5 c), the dc side voltage is regulated to be 1 pu even without that two internal-energy related controls (*modified* horizontal balancing/vertical balancing control) activated. This implies that the external energy dynamics and internal energy dynamics are decoupled from each others, MMC is acting as an energy buffer and its internal energy imbalance does not affect the external active power exchange in between ac and dc side. At  $t = 0.5$  sec., the *modified* horizontal balancing controller is activated. The per-phase stored energy difference between three phases is eliminated within 0.2 sec as shown in Fig. 5 d). At  $t = 1$  sec., the classic vertical balancing controller is activated, driving the energy difference between upper and lower arm to 0 (Fig. 5 e)).

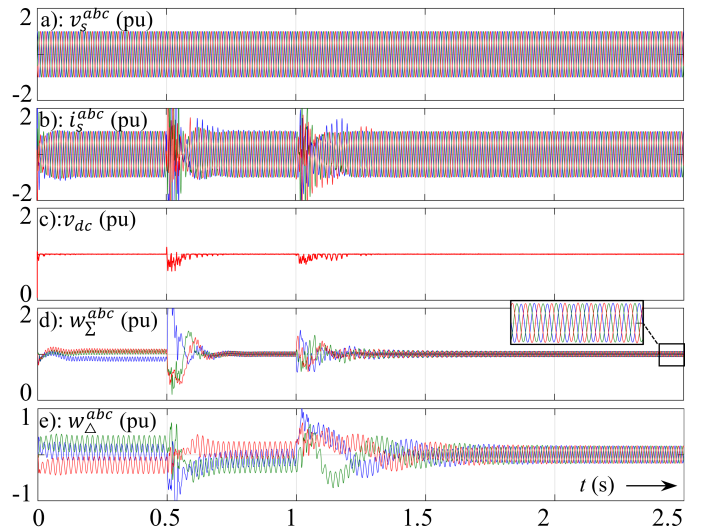


Fig. 5. Simulated Responses for the energy-controlled GFL-MMC

### B. Frequency-domain Analysis

To further verify that the internal energy dynamics have been effectively decoupled from the MMC's external response

based on the proposed control scheme, Fig. 6 compares the output impedance of GFL-MMC with the proposed energy control scheme and a non-energy-controlled GFL-MMC. For comparison purpose, the classic dc voltage control of non-energy controlled MMC is tuned to have the same bandwidth and phase margin as total stored energy control; the PLL, ac current and circulating current control are designed to give the same bandwidth and phase margin as presented in Table. I. With the proposed control scheme, the internal energy-related dynamics are eliminated in both sub- and near-synchronous range, especially that two resonant peaks (as pointed out in Fig. 6 by black arrows) on the magnitude of non-energy controlled GFL-MMC, making it less likely interact with grid impedance. In addition, the proposed control makes MMC passive below 20 Hz, thereby eliminates the negative damping induced by internal energy-related dynamics and avoids associated oscillations in that frequency range. As an additional verification, this frequency-domain analysis shows that the MMC's internal energy-related dynamics are decoupled from its external behavior.

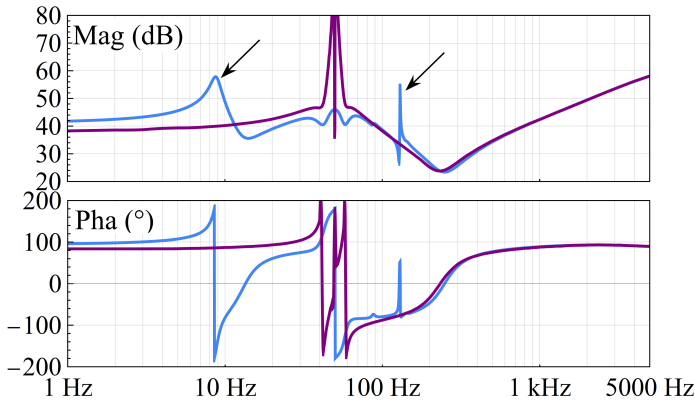


Fig. 6. Output-impedance responses of: non-energy-controlled GFL-MMC with classic control (blue) against energy-controlled MMC with proposed control scheme (purple)

## V. CONCLUSION AND FUTURE WORK

The paper introduces a novel decoupled energy control method for GFL-MMCs that can treat separately internal energy-related dynamics and external energy characteristic (i.e. power transferring). Together with *classic* vertical balancing controller, a *modified* horizontal balancing controller makes the GFL-MMC work as an energy buffer, similar to a dc-bus capacitor in a 2L-VSC. For the purpose of regulating the voltage on the dc-bus in GFL-MMC, the proposed total stored energy controller acts similarly to a conventional dc-bus voltage controller in a 2L-VSC. As a result, the internal energy-related dynamics (regulated by the *modified* horizontal balancing controller and the vertical balancing controller), is completely decoupled from its external energy dynamics (regulated by the total stored energy controller), being regulated separately. In contrast to other energy control methods for GFL-MMC, the proposed control structure controls dc-bus voltage without interfering with internal energy balancing

variables. The time-domain simulation and frequency-domain analysis validates the effectiveness of proposed decoupled energy control. Future works will focus on frequency-domain modeling of the energy-controlled GFL-MMC with the proposed control scheme for stability and fault analysis.

## REFERENCES

- [1] C. Mishra, et al., and L. Vanfretti, "Analysis of STATCOM oscillations using ambient synchrophasor data in Dominion Energy," in *2022 IEEE Power and Energy Society Innovative Smart Grid Technologies Conference (ISGT)*, pp. 1–5, 2022.
- [2] A. António-Ferreira, C. Collados-Rodríguez, and O. Gomis-Bellmunt, "Modulation techniques applied to medium voltage modular multilevel converters for renewable energy integration: A review," *Electric Power Systems Research*, vol. 155, pp. 21–39, 2018.
- [3] A. Antonopoulos, L. Ångquist, L. Harnefors, K. Ilves, and H.-P. Nee, "Global asymptotic stability of modular multilevel converters," *IEEE Transactions on Industrial Electronics*, vol. 61, no. 2, pp. 603–612, 2014.
- [4] N. A. Khan, L. Vanfretti, W. Li, and A. Haider, "Hybrid nearest level and open loop control of modular multilevel converters," in *2014 16th European Conference on Power Electronics and Applications*, pp. 1–12, 2014.
- [5] E. Prieto-Araujo, A. Junyent-Ferré, C. Collados-Rodríguez, G. Clariana-Colet, and O. Gomis-Bellmunt, "Control design of modular multilevel converters in normal and AC fault conditions for HVDC grids," *Electric Power Systems Research*, vol. 152, pp. 424–437, 2017.
- [6] S. Samimi, F. Gruson, X. Guillaud, and P. Delarue, "Control of DC bus voltage with a modular multilevel converter," in *2015 IEEE Eindhoven PowerTech*, pp. 1–6, 2015.
- [7] E. Sánchez-Sánchez, E. Prieto-Araujo, and O. Gomis-Bellmunt, "The role of the internal energy in MMCs operating in grid-forming mode," *IEEE Journal of Emerging and Selected Topics in Power Electronics*, vol. 8, no. 2, pp. 949–962, 2020.
- [8] M. Basić, S. Milovanović, and D. Dujčić, "Comparison of two modular multilevel converter internal energy balancing methods," in *2019 20th International Symposium on Power Electronics (Ee)*, pp. 1–8, 2019.
- [9] S. Fan, K. Zhang, J. Xiong, and Y. Xue, "An improved control system for modular multilevel converters with new modulation strategy and voltage balancing control," *IEEE Transactions on Power Electronics*, vol. 30, no. 1, pp. 358–371, 2015.
- [10] E. Sánchez-Sánchez, E. Prieto-Araujo, A. Junyent-Ferré, and O. Gomis-Bellmunt, "Analysis of MMC energy-based control structures for VSC-HVDC links," *IEEE Journal of Emerging and Selected Topics in Power Electronics*, vol. 6, no. 3, pp. 1065–1076, 2018.
- [11] G. Bergna, J. A. Suul, and S. D'Arco, "Impact on small-signal dynamics of using circulating currents instead of ac-currents to control the DC voltage in MMC HVDC terminals," in *2016 IEEE Energy Conversion Congress and Exposition (ECCE)*, pp. 1–8, 2016.
- [12] T. Li, A. M. Gole, and C. Zhao, "Harmonic instability in MMC-HVDC converters resulting from internal dynamics," *IEEE Transactions on Power Delivery*, vol. 31, no. 4, pp. 1738–1747, 2016.
- [13] J. Lyu, X. Cai, and M. Molinas, "Sub-synchronous oscillation mechanism and its suppression in MMC-based HVDC connected wind farms," *IET Generation, Transmission and Distribution*, vol. 12, no. 4, pp. 1021–1029, 2018.
- [14] H. Wu and X. Wang, "Dynamic impact of zero-sequence circulating current on modular multilevel converters: Complex-valued AC impedance modeling and analysis," *IEEE Journal of Emerging and Selected Topics in Power Electronics*, vol. 8, no. 2, pp. 1947–1963, 2020.
- [15] K. Ji, H. Pang, Y. Li, Z. He, P. Huang, C. Chen, and G. Tang, "A hierarchical small-signal controller stability analysis method for the MMCs," *IEEE Transactions on Power Delivery*, vol. 37, no. 4, pp. 2587–2598, 2022.
- [16] K. Sharifabadi, L. Harnefors, H.-P. Nee, S. Norrga, and R. Teodorescu, *Design, Control, and Application of Modular Multilevel Converters for HVDC Transmission Systems*, pp. 133–213. IEEE, 2016.
- [17] P. Huang and J. Son, "Mitigation of MMC high-frequency resonance by narrowband damping," in *2021 IEEE 22nd Workshop on Control and Modelling of Power Electronics (COMPEL)*, pp. 1–7, IEEE, 2021.
- [18] Q. Tu and Z. Xu, "Impact of sampling frequency on harmonic distortion for modular multilevel converter," *IEEE Transactions on Power Delivery*, vol. 26, no. 1, pp. 298–306, 2011.